

## Magnetization Studies of High $J_c$ Nb<sub>3</sub>Sn Strands

L. Cooley

January 2005

Superconducting Magnet Division  
**Brookhaven National Laboratory**

**U.S. Department of Energy**

USDOE Office of Science (SC), High Energy Physics (HEP) (SC-25)

Notice: This technical note has been authored by employees of Brookhaven Science Associates, LLC under Contract No. DE-AC02-98CH10886 with the U.S. Department of Energy. The publisher by accepting the technical note for publication acknowledges that the United States Government retains a non-exclusive, paid-up, irrevocable, world-wide license to publish or reproduce the published form of this technical note, or allow others to do so, for United States Government purposes.

## **DISCLAIMER**

This report was prepared as an account of work sponsored by an agency of the United States Government. Neither the United States Government nor any agency thereof, nor any of their employees, nor any of their contractors, subcontractors, or their employees, makes any warranty, express or implied, or assumes any legal liability or responsibility for the accuracy, completeness, or any third party's use or the results of such use of any information, apparatus, product, or process disclosed, or represents that its use would not infringe privately owned rights. Reference herein to any specific commercial product, process, or service by trade name, trademark, manufacturer, or otherwise, does not necessarily constitute or imply its endorsement, recommendation, or favoring by the United States Government or any agency thereof or its contractors or subcontractors. The views and opinions of authors expressed herein do not necessarily state or reflect those of the United States Government or any agency thereof.

# Magnetization studies of high $J_c$ Nb<sub>3</sub>Sn strands

A. K. Ghosh, L. D. Cooley, A. R. Moodenbaugh,  
J. A. Parrell, M. B. Field, Y. Zhang, and S. Hong

**Abstract**— Magnetization measurements have been made on several high  $J_c$  Nb<sub>3</sub>Sn strands fabricated by different internal-Sn designs. In general these conductors have high magnetization at low fields, often exhibiting flux-jumps that are characteristic of large superconductor diameter. The effective filament size  $d_{eff}$  is approximately the size of the sub-element because the filament pack within each sub-element is fully coupled. Dividing the filament pack of the sub-element by adding Ta is effective for reducing  $d_{eff}$  and magnetization instability. But, some residual coupling across the dividers seems to remain below 6 K, perhaps due to Ta<sub>3</sub>Sn. Implications for accelerator magnets are discussed.

**Index Terms**—Effective filament diameter, magnetization measurement, niobium-tin compounds, superconducting filaments and wires

## INTRODUCTION

THE requirements of high-field magnets (12-16 T) suitable for high energy particle accelerators has pushed up the critical current density  $J_c$  of Nb<sub>3</sub>Sn wires. At present this limit is about 3000 A/mm<sup>2</sup> within the non-copper region of the wire at 12 T and 4.2 K. Oxford Instruments - Superconducting Technology (OI-ST) has been at the forefront of development, achieving this record  $J_c$  in internal-Sn strand designs using the restacked-rod process (RRP) [1]. Earlier OI-ST also developed high  $J_c$  (>2000 A/mm<sup>2</sup>) using the patented Modified Jelly Roll (MJR) method, which employs a coiled Nb mesh instead of extruded Nb rods [2]. In both cases, these high current densities were a result of designing sub-elements with high Nb-alloy and Sn area, while simultaneously reducing the Cu content to minimal levels and surrounding each sub-element with its own Nb diffusion barrier. A side-effect of this design is the unavoidable coalescence of the Nb filaments during reaction to form a continuous region of Nb<sub>3</sub>Sn. In addition, the barrier is allowed to react, adding a second continuous current-carrying region. Figure 1 shows the reacted sub-elements of a RRP strand at 0.8 mm diameter, which resemble continuous tubes. Furthermore, depending on the duration of reaction at 650-700 °C, and in sections where the barrier has thinned during wire-drawing, the reaction can penetrate through to the copper outside the barrier. All of these features

contrast with those of lower- $J_c$  (~750 A/mm<sup>2</sup>) low-loss wires developed for fusion magnets (*e.g.*, ITER), where the Nb and Sn content are kept low and the diffusion barrier is usually Ta.

The increase in  $J_c$  has thus come at the expense of large superconductor dimension. With the number of sub-elements  $N = 54$ , and with 50% copper stabilizer, a typical sub-element diameter  $d_N$  is ~80 μm. This leads to magnetization values that are two orders of magnitude higher than for typical Nb-Ti accelerator magnet conductors, which may produce unacceptably large error fields. In a separate paper we show that the flux-jumps lead to a “magnetic” instability at low fields in these strands carrying transport currents [3].

In this paper we describe some magnetization measurements of internal-Sn strands produced by the MJR and RRP process, and explore one option of reducing the magnetization by incorporating Ta to sub-divide the tube-like reacted superconductor.

## I. SAMPLE PREPARATION AND MEASUREMENT PROCEDURES

Samples of wire ~ 30 cm long were reacted in vacuum. All samples were given the same initial steps of 48 h at 210 °C followed by 48 h at 400 °C. Final reaction temperatures were 665 °C +/- 10 °C for times ranging from 72-180 h, the temperature varying downward from the reference thermocouple with higher mass loaded into the furnace. At the same time, samples for critical current ( $I_c$ ) measurements were reacted separately, as described elsewhere [4]. After reaction, a hexagonal bundle of 7 wires were potted in epoxy and cut using a diamond saw to a length of 6 mm. A typical wire twist pitch used to make these 6-around-1 bundles was 13 mm. Note that after reaction the diameters  $D$  of all the strands increased by approximately 5-6%. However,  $J_c$  is calculated using the un-reacted strand diameter and non-copper fraction.

Magnetization and susceptibility measurements were made with a commercial SQUID magnetometer with the field

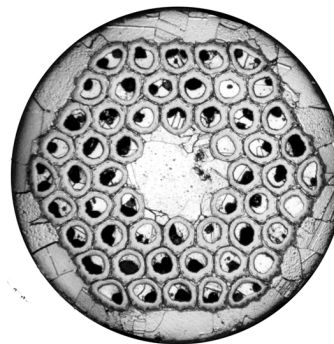


Fig. 1 A cross section of a reacted Nb<sub>3</sub>Sn internal-Sn strand with  $J_c$  of ~3000 A/mm<sup>2</sup>. Rings of Nb<sub>3</sub>Sn surround the former location of solid tin. Grain boundaries in the copper matrix are also evident.

Manuscript received October 5, 2004.

This work was supported in part by the U.S. Department of Energy under Contract No. DE-AC02-98CH10886.

AKG, LDC, and ARM are affiliated with Brookhaven National Laboratory, Upton, NY 11973 USA (phone: 631-344-3974; fax: 631-344-2190; e-mail: aghosh@bnl.gov).

JAP, MBF, YZ, and SH are with Oxford Superconducting Technology, Carteret, NJ, USA

TABLE I  
STRAND PARAMETERS

| Sample | Billet   | Final HT     | $\Delta M$ (3 T)<br>kA/m | Non-Cu % | $D$<br>mm | $N$ | $d_N$<br>$\mu\text{m}$ | $J_c(12\text{ T})$<br>A/mm <sup>2</sup> | $J_e(12\text{ T})$<br>A/mm <sup>2</sup> | $J_c(3\text{ T})$<br>A/mm <sup>2</sup> | $d_{\text{eff}}$<br>$\mu\text{m}$ |
|--------|----------|--------------|--------------------------|----------|-----------|-----|------------------------|---|---|--|-----------------------------------|
| A      | MJR 202  | 675°C / 72h  | 173.6                    | 38.5     | 0.80      | 42  | 77                     | 1948                                    | 729                                     | 4027                                   | 102                               |
| B      | MJR 163  | 675°C / 180h | 177.6                    | 39.5     | 0.80      | 42  | 78                     | 1812                                    | 688                                     | 3881                                   | 108                               |
| C      | RRP 7054 | 675°C / 180h | 254.9                    | 50.0     | 0.70      | 54  | 68                     | 2655                                    | 1266                                    | 5797                                   | 104                               |
| D      | RRP 7054 | 665°C / 72h  | 273.1                    | 50.0     | 0.70      | 54  | 68                     | 2899                                    | 1449                                    | 7045                                   | 91                                |
| E      | RRP 7260 | 665°C / 72h  | 124.7                    | 51.2     | 0.90      | 54  | 88                     | 1966                                    | 1007                                    | 5555                                   | 53                                |
| F      | RRP 7260 | 675°C / 180h | 103.6                    | 51.2     | 0.90      | 54  | 88                     | 2046                                    | 1004                                    | 5783                                   | 42                                |
| G      | RRP 7261 | 665°C / 72h  | 313.4                    | 51.7     | 0.90      | 54  | 88                     | 2320                                    | 1148                                    | 6858                                   | 108                               |
| H      | RRP 7261 | 675°C / 180h | 305.1                    | 51.7     | 0.90      | 54  | 88                     | 2491                                    | 1220                                    | 72886                                  | 99                                |

transverse to the wire bundle. The background solenoid (maximum field 5 T) was in persistent mode during the measurement and field steps are made with no overshoot. Hysteresis loops were acquired at 4.5 K using a typical field step of 0.1 T. Widths of hysteresis loops  $\Delta M$  at 3 T field were calculated using the total wire volume. The susceptibility of the sample was measured while warming in a 10 mT field after having been cooled to 4.5 K in zero-field.

Critical current measurements were made at 8-11.5 T at BNL and at higher fields at OI-ST. Besides the 12 T  $J_c$  for the non-Cu region, we also determine the “engineering” current density  $J_e$  as the equivalent current density within the total wire cross-section. We extrapolate using an exponential fit to estimate  $J_e$  at the 3 T fields where  $\Delta M$  was determined, and these values of  $J_e$  and  $\Delta M$  were used to calculate the effective filament diameter  $d_{\text{eff}}$  [5] from the critical state model:

$$d_{\text{eff}} = (3\pi/4)\Delta M / J_e \quad (1)$$

Note that  $d_{\text{eff}}$  is only a representation of the magnetization and is used to gauge the multifilamentary nature of the composite. For internal-Sn  $\text{Nb}_3\text{Sn}$  wires, this  $d_{\text{eff}}$  is always larger than the individual filament diameter prior to reaction, which is indicative of filament bridging [5-7]. In the present case, where the filaments coalesce into a tube of superconductor, it is comparable to the sub-element diameter  $d_N$ .

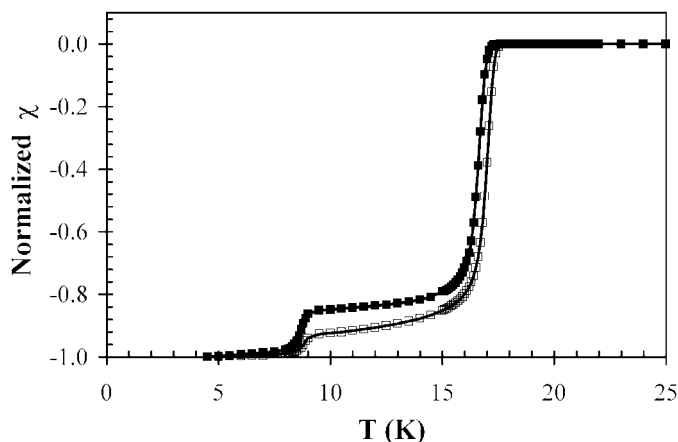


Fig. 2 Plot shows the normalized susceptibility versus temperature for samples A (triangles) and B (filled circles). The 9 K transition is that of the un-reacted Nb-barrier.

## II. MEASUREMENTS

Table I presents a summary of the different wires that were measured and the results that were obtained. Samples A and B have the same design features, whereas sample C and D are the newer high  $J_c$  RRP design. Samples D and E are from a billet with Ta-dividers, G and H are from a control billet without the dividers, and in these billets the tin-content is reduced to match the niobium content in the filament pack. The longer reaction times are usually used by OS-IT to optimize  $J_c$ . However, recent studies have shown that comparable  $J_c$  can be obtained with shorter times. This is discussed in subsequent sections.

### A. MJR-Type wire

Figure 2 shows the susceptibility of wires from two MJR billets with different reaction times. The shoulder before the transition at 9 K shows that for longer times the Nb-barrier is more fully reacted. For the long reaction times, the barrier, which is not always uniform, can be breached where it is thin, allowing Sn to leak into the stabilizing Cu and resulting in a much lower  $RRR$  (the ratio of resistance at 295 K to that at 18 K). For instance, sample B has an  $RRR$  of 3 compared to 61 for sample A. However, the magnetization of the two wires is fairly similar, as shown in Fig. 3. A common feature of all the wires is the observation of flux jumps at low fields [8-10], which in Fig. 3 is seen below 1 T. Note that sample A is cycled from positive to negative fields, whereas sample B is only

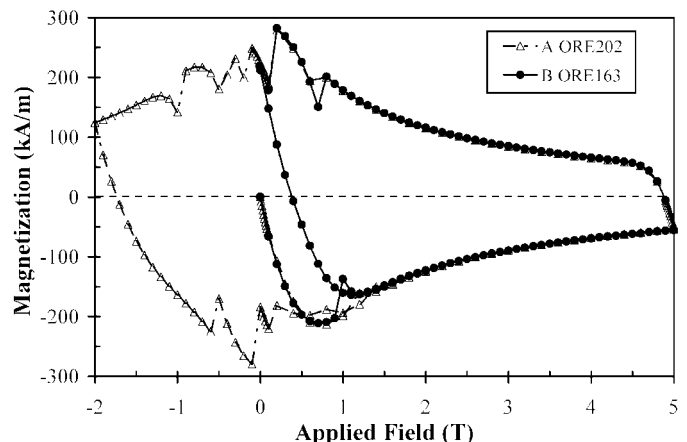


Fig. 3 Volume magnetization of sample A and B at 4.5 K. Drop in magnetization is an indication of flux-jump. Since measurements are taken at intervals, the extent of the drop is hidden by the re-magnetization after the flux-jump.

cycled through positive fields as a conductor in a magnet would be. This can produce different flux-jump behavior.

### B. RRP-Type wire

The 0.7mm diameter RRP wires from billet 7054 have a higher percentage of Nb and Sn in the sub-element as compared to the MJR wires, as discussed earlier. Consequently the  $J_c$  at 12 T is also higher, and larger magnetization and flux-jump instabilities up to 1.5 T are found. In this case, reaction times of 72 h were sufficient to fully react the barrier with the wire having a  $J_c(12\text{ T})$  of 2900 A/mm<sup>2</sup>. For longer times, the  $J_c$  and the RRR of the wire drops. Fig. 4 shows the magnetization of the two wires from billet 7054.

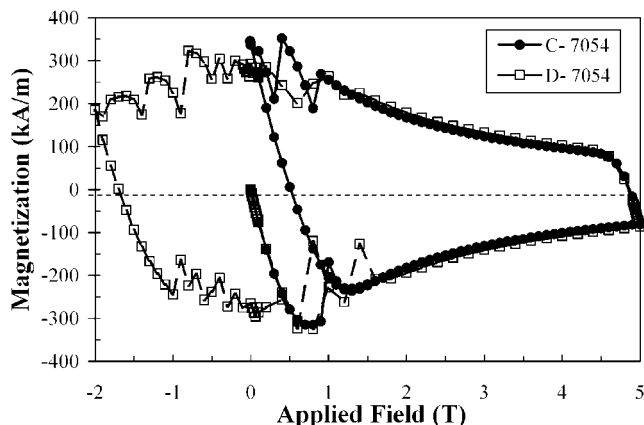


Fig. 4. Plot of magnetization at 4.5 K for samples C and D.

### C. RRP-Type wires with Ta divider

One way to reduce magnetization and hence  $d_{eff}$  in the strand is to introduce non-superconducting internal barriers to divide the filament pack in the sub-element. Zeitlin *et al.* have used Nb60wt%Ta fins to separate the Nb filament array with some success [11]. In OI-ST's innovative strand design (Billet 7260), copper clad Ta rods were used to split the filament pack into six approximately rectangular regions, and Ta sheet was placed against the Nb-barrier to prevent it from reacting and forming a continuous ring of Nb<sub>3</sub>Sn, as shown in Fig. 5. Light microscopy analyses, as exemplified in Fig. 5, indicated that the Ta filament spokes indeed seemed to divide the reacted Nb<sub>3</sub>Sn area, while the Ta sheet seemed to likewise be effective for preventing barrier reaction.

This scheme appears to have been quite successful at

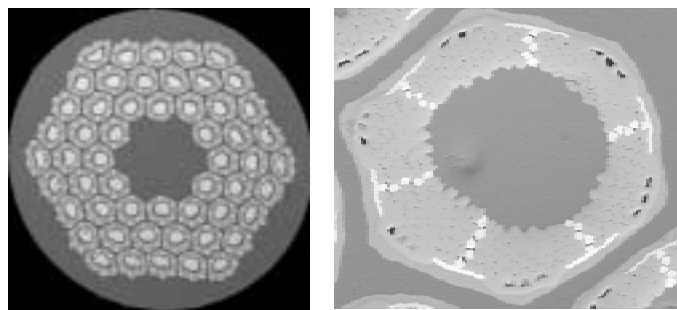


Fig. 5 Photomicrographs of un-reacted 0.8 mm wire from billet 7260. A reacted sub-element is shown at the right

achieving the intended electromagnetic changes as well: The magnetization of samples F and H, which were reacted for 180 h at 675 °C and should have full coupling if it is to emerge, are compared in Fig. 6. This shows an obvious reduction in the overall magnetization and the field at which flux jumps appear. In Figs. 7 it is obvious that this suppression occurs throughout the superconducting state, indicating that indeed the length scale for the dimension of the superconductor has been reduced closer to the adiabatic threshold. In Table I, both samples E and F exhibit clear reduction in the value of  $d_{eff}$  over their counterparts, samples G and H respectively.

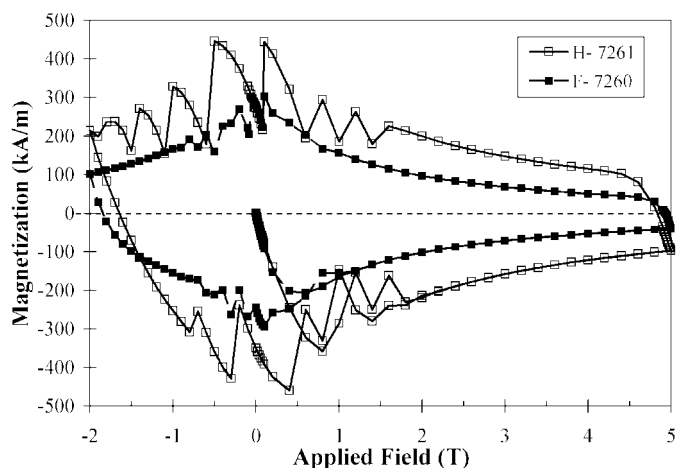


Fig. 6. Volume magnetization of samples F and H as a function of field at 4.5 K. As magnetization decreases the incidence of flux-jumping also decreases.

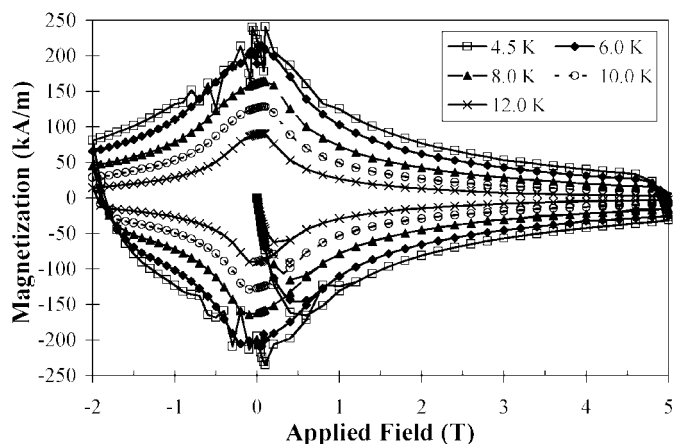


Fig. 7. A plot of magnetization vs. field for sample F at different temperatures. No flux jumps are observed above 6 K.

One consequence of introducing dividers and barriers is that they take up part of the non-copper area that could be used for Nb<sub>3</sub>Sn, and hence the  $J_c$  of the composite will be lower. This assumes of course that the critical current density within the Nb<sub>3</sub>Sn itself is maintained at a constant level. Compared to a control billet (7261) made without these modifications, the expected  $J_c$  reduction for billet 7260 is ~15%, as indicated in Table I for both final reactions studied.

Sumption *et al.* [12] have calculated the effect of subdivisions on the magnetization of a superconducting cylinder. These calculations estimate that the magnetization for wires

from 7260 would be a factor of 5 lower than that of wires from billet 7261. However, while our data show a lower magnetization for billet 7260, the reduction in magnetization at 4.5 K is only a factor of 3. We speculate that the divided  $\text{Nb}_3\text{Sn}$  filament packs are still coupled by narrow regions of superconductor with a lower critical temperature  $T_c$ . Such a region should produce an extra contribution to the magnetization, but might not contribute to the transport  $J_c$ . In particular,  $\text{Ta}_3\text{Sn}$  has a  $T_c$  of  $\sim 7$  K and an upper critical field of  $\sim 5$  T at 4.5 K [13].

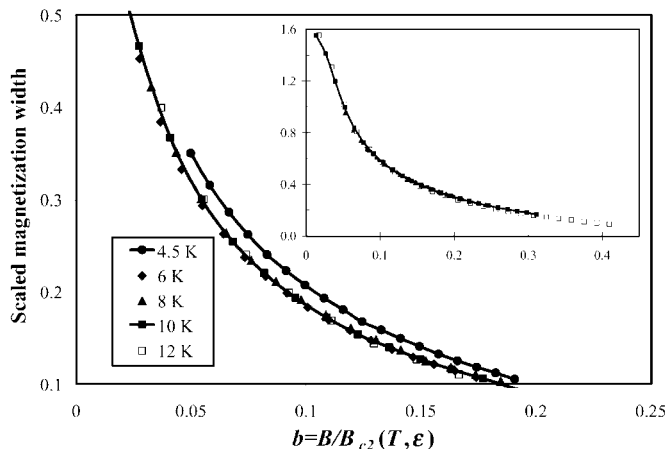


Fig. 8 Plot of the scaled magnetization width for sample F (Ta-divided) as a function of the reduced field  $b$ . Inset shows the same plot for sample H (from the control billet).

To explore this possibility, the magnetization was measured at 6, 8, 10, and 12 K. This is shown in Fig. 7 for sample F. From these measurements, we scale  $\Delta M$  ( $\propto J_c$ ) as a function of reduced field  $b = B/B_{c2}(T, \epsilon)$  at the different reduced temperatures  $t = T/T_c$  using Summer's formulation [14]:

$$\Delta M_S = C(\Delta M)B_{c2}(T, \epsilon)^{1/2}(1-t^2)^2. \quad (2)$$

Here  $B_{c2}$  is the upper critical field, expressed with its temperature  $T$  and strain  $\epsilon$  dependence,  $B$  is the applied field,  $t = T/T_{c0}(\epsilon)$ ,  $T_{c0}(\epsilon)$  is the critical temperature in zero field, and  $C$  is a scaling coefficient independent of temperature and field. The following parameters were used: strain  $\epsilon = -0.0016$ ,  $B_{c2} = 28.5$  T, and  $T_{c0} = 17.8$  K for Sample F and 18.3 K for sample H, respectively. The result of this scaling analysis is shown in Fig. 8. Notice that the data set at 4.5 K lie off of the scaling curve, which is evidence that an additional component of magnetization contributes to those data. This could indeed be due to  $\text{Ta}_3\text{Sn}$ . By contrast, sample H from billet 7261, which received the same reaction but does not incorporate tantalum, shows good scaling with temperature for magnetization widths at 4.5, 6.0, 8.0, 10.0, and 12.0 K (inset in Fig. 8).

### III. CONCLUSION

In present  $\text{Nb}_3\text{Sn}$  strand designs, high  $J_c$  has been achieved at the expense of large magnetization and flux-jump instability. This magnetic instability can, at low fields, give rise to unpredictable error fields in magnets, hence for accelerator

high field magnets it is desirable to have  $d_{eff}$  less than  $\sim 40$   $\mu\text{m}$ . Moreover, the tendency to initiate flux jumps at low fields makes those sections of magnets prone to quench, even though the operating current might be well below the critical current in the high-field regions of the magnet.

The use of Ta dividers is effective for reducing the magnetization in these strands. However at 4.5 K, there appears to be some residual coupling of the divided filament sections, which could be due to  $\text{Ta}_3\text{Sn}$ . This leads to higher than expected magnetization there. Otherwise, the divided strands produce the desired reduction in superconductor dimension. It is possible that with further refinements of this design, strands could be made that meet the 40  $\mu\text{m}$   $d_{eff}$  goal. It is also significant that  $J_c$  too has been reduced due to the loss of  $\text{Nb}_3\text{Sn}$  area. Hence R&D should be made to further increase the critical current density of the  $\text{Nb}_3\text{Sn}$  layer itself.

### ACKNOWLEDGMENT

A. K. Ghosh thanks A. Werner and R. Sikora for heat treating the samples, and E. Sperry for his expert help in measuring the critical current of the strands.

### REFERENCES

- [1] J. A. Parrell, M. B. Field Y. Zhang and S. Hong, "Nb<sub>3</sub>Sn conductors development for fusion and particle accelerator applications", *Adv. in Cryo. Eng.*, vol. 50, ed. U. Balachandran, pp. 369-375, 2004.
- [2] J. A. Parrell, Y. Zhang, R. W. Hentges, M. B. Field and S. Hong, "Nb<sub>3</sub>Sn strand development at Oxford Superconducting Technology", *IEEE Trans. Appl. Supercond.*, vol. 13, pp. 3470-3473, June 2003.
- [3] A. K. Ghosh, L. D. Cooley, and A. Moodenbaugh, "Investigation of instability in high  $J_c$  Nb<sub>3</sub>Sn strands", to be presented at this conference, paper 2MB03.
- [4] R. Soika, L. D. Cooley, A. K. Ghosh, A. Werner, "Fixture for testing of modern high energy physics Nb<sub>3</sub>Sn strands", *Adv. in Cryo. Eng.*, vol. 50, ed. U. Balachandran, pp. 67-74, 2004
- [5] A. K. Ghosh, K. E. Robins and W. B. Sampson, "Magnetization measurements on multifilamentary Nb<sub>3</sub>Sn and NbTi conductors", *IEEE Trans. Magnetics*, vol. 21, pp. 328-331, March 1985.
- [6] R. B. Goldfarb and J. W. Ekin, *Cryogenics* 26, pp. 478, 1986.
- [7] A. K. Ghosh and M. Suenaga, "Magnetization and critical currents of Sn-core multifilamentary Nb<sub>3</sub>Sn conductors", *IEEE Trans. Magnetics*, vol. 27, pp. 2407-2410, March 1991.
- [8] E. Barzi, P. J. Limon, R. Yamada and A. V. Zlobin, "Study of Nb<sub>3</sub>Sn strands for Fermilab's high field dipole magnets" *IEEE Trans. Appl. Supercond.*, vol. 11, pp. 3595-3598, March 2001.
- [9] R. B. Goldfarb, L. F. Goodrich, T. Pyon and E. Gregory, "Suppression of flux jumps in marginally stable Niobium-Tin superconductors", *ibid.* pp. 3679-3682.
- [10] M. D. Sumption, X. Peng, E. Lee, X. Wu and E. W. Collings, "Analysis of magnetization, AC loss, and  $d_{eff}$  for various internal-Sn based Nb<sub>3</sub>Sn multifilamentary strands with and without subelement splitting", *Cryogenics*, Vol. 44, October 2004, pp 711-725.
- [11] B. A. Zeitlin, *et al.*, "Progress in the use of internal fins as barriers to reduce magnetization on high current density mono-element internal Tin conductors (MEIT)", *Adv. in Cryo. Eng.*, vol. 50, ed. U. Balachandran, pp. 417-424, 2004
- [12] M. D. Sumption, X. Peng and E. W. Collings, "Magnetization and  $d_{eff}$  in HEP relevant RIT type Nb<sub>3</sub>Sn strands-influence of internal barriers", *ibid.*, pp. 836-843, 2004.
- [13] G. Otto, "Preparation and properties of Ta-Sn and Nb-Ge diffusion layers", *J. Appl. Phys.* vol. 42, p. 57, 1971.
- [14] L. T. Summers, M. W. Guinan, J. R. Miller, and P. A. Hahn, "A Model for the prediction of Nb<sub>3</sub>Sn critical current as a function of field, temperature, strain, and radiation damage", *IEEE Trans. Magnetics*, vol. 27, pp. 2041-2044, March 1991.